

# Evaluation of $E$ - $J$ Characteristics of YBCO Coated Conductor in a Wide Range of Electric Field

K. Yamauchi<sup>a,1</sup>, M. Kiuchi<sup>a</sup>, E.S. Otabe<sup>a</sup>, T. Matsushita<sup>a</sup>,  
T. Kuga<sup>b</sup>, M. Inoue<sup>b</sup>, T. Kiss<sup>b</sup>, Y. Iijima<sup>c</sup>, K. Kakimoto<sup>c</sup>  
T. Saitoh<sup>c</sup>

<sup>a</sup> Faculty of Computer Science and Systems Engineering, Kyushu Institute of Technology, 680-4 Kawazu, Iizuka 820-8502, Japan

<sup>b</sup> Department of Electrical and Electronic Systems Engineering, Graduate School of Information Science and Electrical Engineering, Kyushu University, 6-10-1 Hakozaki, Higashi-ku, Fukuoka 812-8581, Japan

<sup>c</sup> Fujikura Ltd., 1-5-1 Kiba, Koto-ku, Tokyo 135-8512, Japan

---

## Abstract

The  $E$ - $J$  characteristics were measured for a YBCO-coated conductor by using the four probe method and the relaxation method of DC magnetization. The result on the latter measurement at extremely low electric fields was theoretically analyzed based on the flux creep-flow model. From the result on  $n$ -value the flux lines in YBCO are considered to be in the glass state even at high fields. The apparent pinning potential  $U_0^*$  estimated from the relaxation of DC magnetization is much larger than that of Bi-2223. The present theoretical analysis clarifies a much stronger flux pinning and a higher dimensionality of YBCO in comparison with Bi-2223.

*Keywords:* critical current density, IBAD coated tape, YBCO, flux creep-flow model

*PACS:* 74.60Jg, 74.25.Fy, 74.72.Bk, 74.60.Ge

---

<sup>1</sup> Corresponding author. Postal address: Department of Computer Science and Electronics, Kyushu Institute of Technology, 680-4 Kawazu, Iizuka 820-8502, Japan  
Phone: +81-948-29-7661  
Fax: +81-948-29-7661  
E-mail address: yamauchi@aquarius10.cse.kyutech.ac.jp

## 1 Introduction

YBCO is most promising for a power application because of a superior critical current characteristic at high magnetic fields in various high- $T_c$  superconductors. This characteristic depends on the electric field and the range of electric field that the superconductor experiences is different depending on the kind of application. For example, AC power cable is used in relatively high electric field region, while NMR device is used in extremely low electric field region.

Recently long YBCO coated conductors with high critical current are successfully fabricated. Application of such conductor is really expected. Hence, the evaluation of  $E$ - $J$  characteristics of YBCO coated conductors in a wide range of electric field is necessary. Although the  $E$ - $J$  characteristic at relatively high electric fields is usually measured by resistive method, that in the range of extremely low electric field region has not yet been clarified. Therefore, it is necessary to measure the  $E$ - $J$  characteristic in this electric field region. In this paper, this characteristic is measured by a relaxation method of DC magnetization, and the result is compared with a theoretical analysis based on the flux creep-flow model [1] as well as that in a relatively high electric field region measured by a four probe method. Furthermore, the  $n$ -value and the apparent pinning potential  $U_0^*$ , which characterize the applicability of superconductor, are also evaluated.

## 2 Experimental details

The specimen measured is an YBCO coated wire made by IBAD method. The  $c$ -axis was directed normal to the flat surface of the wire. The specification of

the specimen is shown in Table 1. The magnetic relaxation was measured in a magnetic field along the *c*-axis in a temperature range of 30 ~ 60 K using a SQUID magnetometer (MPMS-7). The magnetic field of sufficient strength was first applied to the specimen, and then reduced to an aimed value, and the relaxation of the magnetic moment, *m*, was measured. The current density, *J*, and the electric field, *E*, are estimated by the following equations [2]:

$$J = \frac{12m}{w^2 d(3l - w)}, \quad (1)$$

$$E = -\frac{\mu_0}{2d(l + w)} \frac{dm}{dt}, \quad (2)$$

where *l* is the length, *w* is the width and *d* is the thickness of specimen. Eq. (2) gives a mean electric field in the specimen for a magnetic field distribution given by Bean's model.

The four probe method was also used in the magnetic field parallel to the *c*-axis to measure the *E-J* characteristics in the range of relatively high electric field in a temperature range of 30 ~ 60 K. The specimen was chemically etched to a shape of a bridge and the dimension of narrow region was 1 mm long and 100  $\mu$ m wide.

### 3 Results and Discussion

The results of both measurements at 40 K and 50 K are shown in Figs. 1 and 2, respectively. The data obtained by the four probe method and the relaxation method of DC magnetization are distributed in the regions of relatively high ( $E = 10^{-3} \sim 10^0$ ) and extremely low ( $E = 10^{-8} \sim 10^{-6}$  V/m) electric field. At 40 K,  $J_c$  is very high at low fields and the resistive measurement could not be performed. At 50 K, a connection between the data obtained by the

two methods is not consistent at low fields. Since the two measurements were consistent in a previous experiment on Bi-2223 tape [3], the reason for the present inconsistency is not clear. Because of this inconsistency, a focus is given on the results of magnetic measurement.

The above result is compared with a theoretical analysis using the flux creep-flow model. According to this model, the  $E$ - $J$  characteristics can be calculated using the pinning potential given by [4]

$$U_0 = \frac{0.835g^2 k_B J_{c0}^{1/2}}{(2\pi)^{3/2} B^{1/4}}, \quad (3)$$

where  $J_{c0}$  is the virtual critical current density in the creep-free case and  $g^2$  is the number of flux lines in the flux bundle. The magnetic field and temperature dependencies of  $J_{c0}$  at low fields are assumed as

$$J_{c0} = A \left[ 1 - \left( \frac{T}{T_c} \right)^2 \right]^m B^{\gamma-1}, \quad (4)$$

where  $A$ ,  $m$  and  $\gamma$  are pinning parameters. Here, it is assumed that  $A$  is distributed as

$$f(A) = K \exp \left[ -\frac{(\log A - \log A_m)^2}{2\sigma^2} \right], \quad (5)$$

where  $A_m$  is the most probable value,  $\sigma^2$  is a constant representing the degree of deviation and  $K$  is a constant.

The value of  $g^2$  is assumed to be determined so that the critical current density under the flux creep might take on a maximum value [5], and is given by

$$g^2 = g_e^2 \left[ \frac{5k_B T}{2U_e} \ln \left( \frac{B a_f \nu_0}{E} \right) \right]^{4/3}, \quad (6)$$

where  $a_f$  is a flux line spacing,  $\nu_0$  is an oscillation frequency of the flux bundle,  $g_e$  is a value of  $g$  when flux lines form a perfect triangular lattice, and  $U_e$  is the value of  $U_0$  when  $g = g_e$ . Strictly speaking,  $g^2$  depends on  $E$  as well as on

$B$  and  $T$ . However, the value of  $g^2 = 1.39$  at  $E = 10^{-10}$  V/m,  $B = 0.3$  T and  $T = 70$  K is approximately used as a typical value in the present calculation [1].

The parameters  $A_m$ ,  $\sigma^2$ ,  $m$  and  $\gamma$  used in the numerical calculation in the whole ranges of temperature and magnetic field are listed in Table 2. These parameters were determined so as to obtain a good agreement between the theoretical and experimental  $E$ - $J$  curves in extremely low electric field region. The results calculated in a wide range of electric field are shown by solid lines in Figs. 1 and 2 to compare with the experimental results. Although the theoretical results disagree with the experimental results of the resistive measurements at relatively high electric field, the observed  $E$ - $J$  characteristics at low electric fields can approximately be explained.

The present result on the YBCO coated conductor is completely different from a previous result on a Bi-2223 tape. In the Bi-2223 tape, the  $E$ - $J$  curve was concave downward showing the typical behavior in the liquid state of flux lines even at low magnetic field such as 0.1 T at 50 K. On the contrary the  $E$ - $J$  curve is concave upward showing that flux lines are in the glass state even at high fields at the same temperature for the YBCO tape. This difference is attributed to the differences in  $A_m$ , and  $g^2$ :  $A_m = 9.0 \times 10^8$  and  $g^2 = 1.39$  in the Bi-2223 tape. The difference of the flux pinning causes the difference of  $A_m$  and the difference of the dimensionality of superconductor causes the difference of the both quantities.

Figs. 3 and 4 show the  $n$ -value in the relatively high and extremely low electric field regions, respectively. At 40 K and 50 K, the  $n$ -value at extremely low electric fields is entirely larger than that at the relatively high electric fields. Therefore, flux lines in the YBCO coated conductor in this temperature region

is the glass state. On the other hand, in the field region above 2 T at 60 K, the  $n$ -value at low electric fields is smaller than that at high electric fields, showing that flux lines are in the liquid state.

The apparent pinning potential  $U_0^*$  is estimated from the relaxation of magnetization:

$$U_0^* = -k_B T \left[ \frac{1}{M_0} \frac{\partial M}{\partial (\log t)} \right], \quad (7)$$

where  $M_0$  is the initial magnetization before the relaxation. The results are shown in Fig. 5.  $U_0^*$  has a sharp maximum at around the reduced temperature ( $T/T_c$ ) of 0.5 in the magnetic field range of the present measurement. This is different from the case of Bi-2223 tape where  $U_0^*$  takes a small peak at a low reduced temperature [6]. Comparing with these figures, the apparent pinning potential  $U_0^*$  for an YBCO wire has bigger potentials than that for Bi-2223 silver-sheathed tape wire. The value of  $U_0^*$  in YBCO tape is much larger than that in Bi-2223 tape, which is lower than 100 meV. This difference is also caused by the difference of the flux pinning strength and the dimensionality of the superconductor.

#### 4 Summary

The  $E$ - $J$  characteristic of the YBCO coated tape is measured in the range of relatively high and extremely low electric fields. This characteristic was successfully explained by the flux creep theory. It is found that the  $E$ - $J$  characteristic is concave upward suggesting the glass state for flux lines even at high fields. This behavior is clearly seen from the  $n$ -value. The apparent pinning potential  $U_0^*$  is larger than 100 meV and is much larger than that of Bi-2223.

## 5 Acknowledgement

This work was supported by New Energy and Industrial Technology Development Organization (NEDO) as Collaborative Research and Development of Fundamental Technologies for Superconducting Applications.

## References

- [1] T. Matsushita, T. Tohdoh, N. Ihara, Physica C **259** (1996) 321.
- [2] T. Nakamura, T. Kiss, Y. Hanayama, T. Matsushita, K. Funaki, M. Takeo, F. Irie, Advances in Superconductivity X, (Springer, Tokyo, 1998) p. 581.
- [3] T. Kodama, M. Fukuda, K. Shiraishi, S. Nishimura, E.S. Otabe, M. Kiuchi, T. Kiss, T. Matsushita, K. Itoh, Physica C **357–360** (2001) 582.
- [4] T. Matsushita, T. Fujiyoshi, K. Toko and K. Yamafuji, Appl. Phys. Lett. **56** (1990) 2039.
- [5] T. Matsushita, Physica C **217** (1993) 461.
- [6] T. Matsushita, M. Kiuchi and Y. Nakayama, Proceeding of International Workshop on Critical Currents in Superconductors for Practical Applications, 1997, p. 40.

Table 1. Specification of specimen.

$T_c$ (K)	$l$ (mm)	$w$ (mm)	$d$ ( $\mu$ m)
87.8	2.74	2.04	1.0

Table 2. Pinning parameters for using numerical calculation.

$B_{c2}(0)$ [T]	$\rho_n(T_c)$ [ $\Omega m$ ]	$A_m$	$\sigma^2$	$\gamma$	$m$	$\zeta$	$g^2$
80.5	$2.0 \times 10^{-6}$	$8.5 \times 10^{10}$	0.009	0.62	3.0	$2\pi$	3

### Figure captions

Fig. 1.  $E$ - $J$  characteristics of YBCO coated conductor at 40 K.

Fig. 2.  $E$ - $J$  characteristics of YBCO coated conductor at 50 K.

Fig. 3.  $n$ -value of YBCO coated conductor at relative high electric field region.

Fig. 4.  $n$ -value of YBCO coated conductor at extremely low electric field region.

Fig. 5. Normalized temperature dependence of apparent pinning potential,  $U_0^*$  of YBCO coated conductor at various magnetic fields

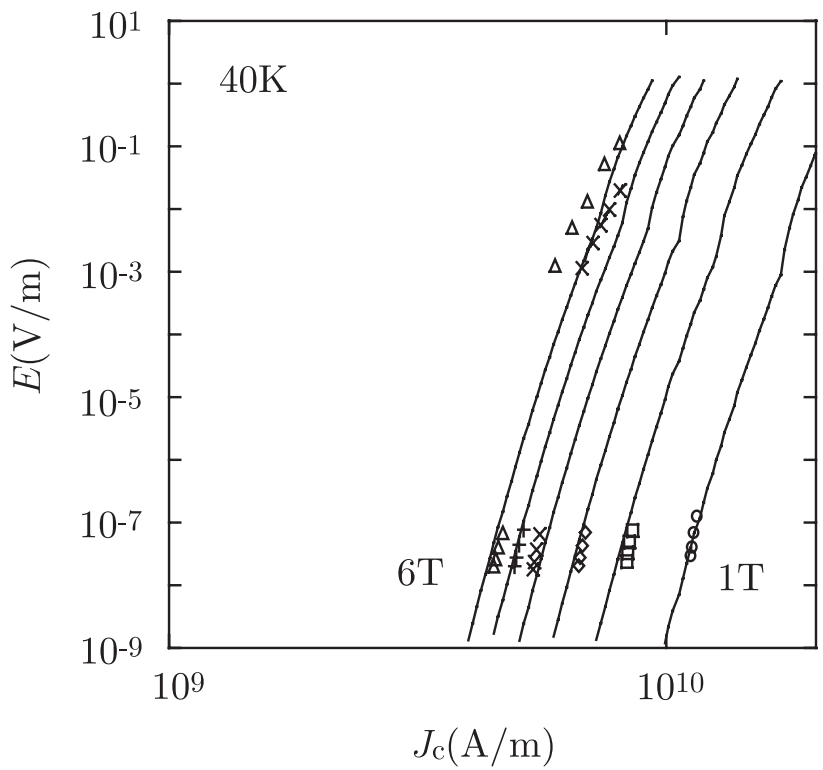


Figure 1: K. Yamauchi *et al.*/WSP-18/ ISS2002

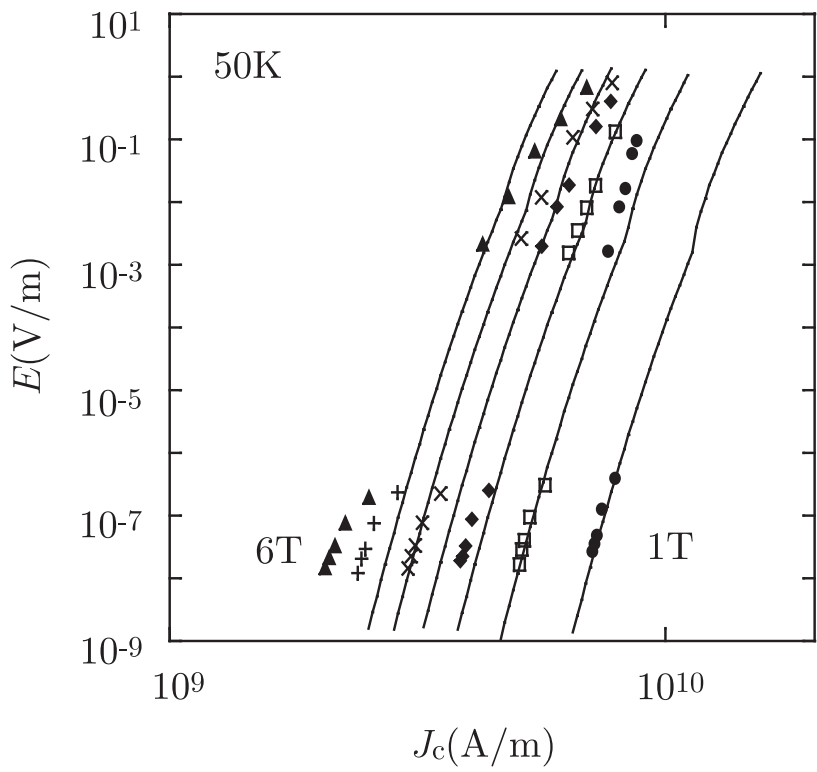


Figure 2: K. Yamauchi *et al.*/WSP-18/ ISS2002

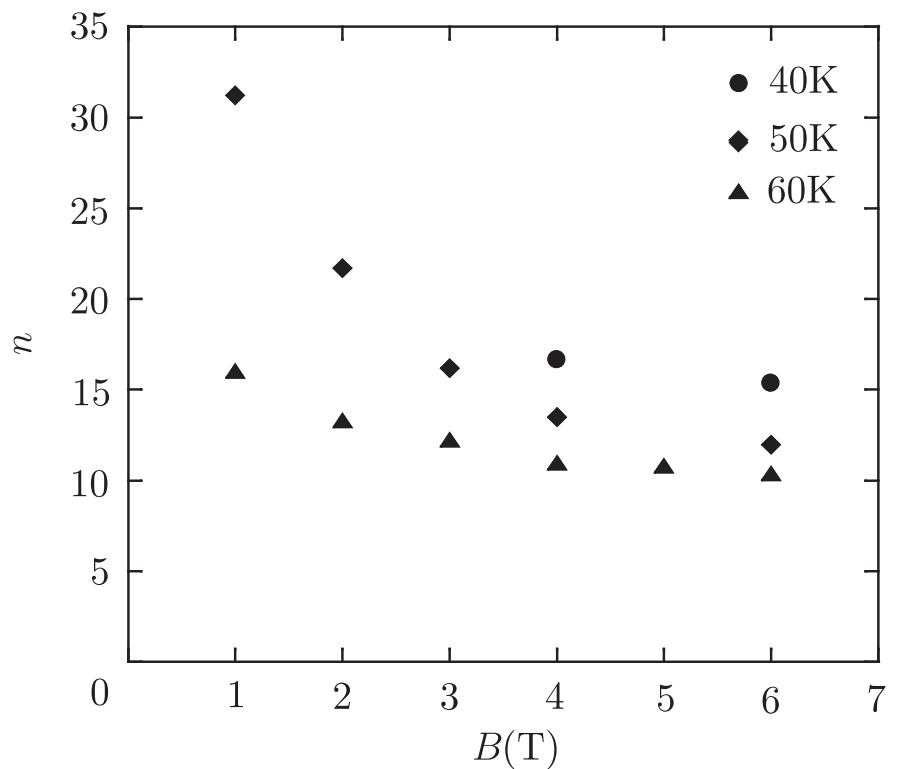


Figure 3: K. Yamauchi *et al.*/WSP-18/ ISS2002

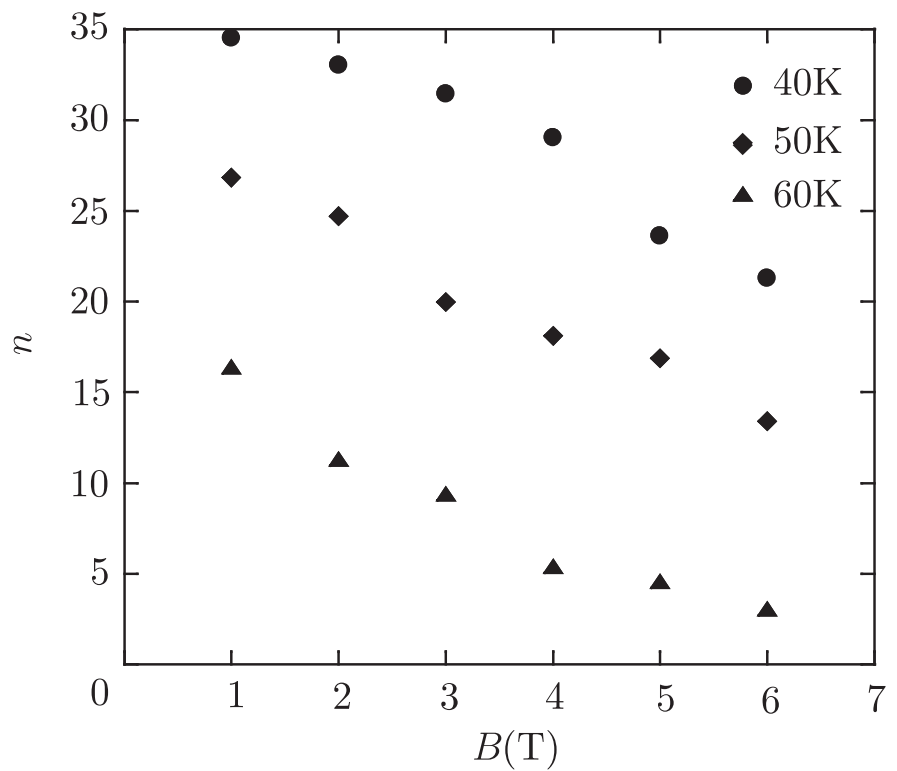


Figure 4: K. Yamauchi *et al.*/WSP-18/ ISS2002

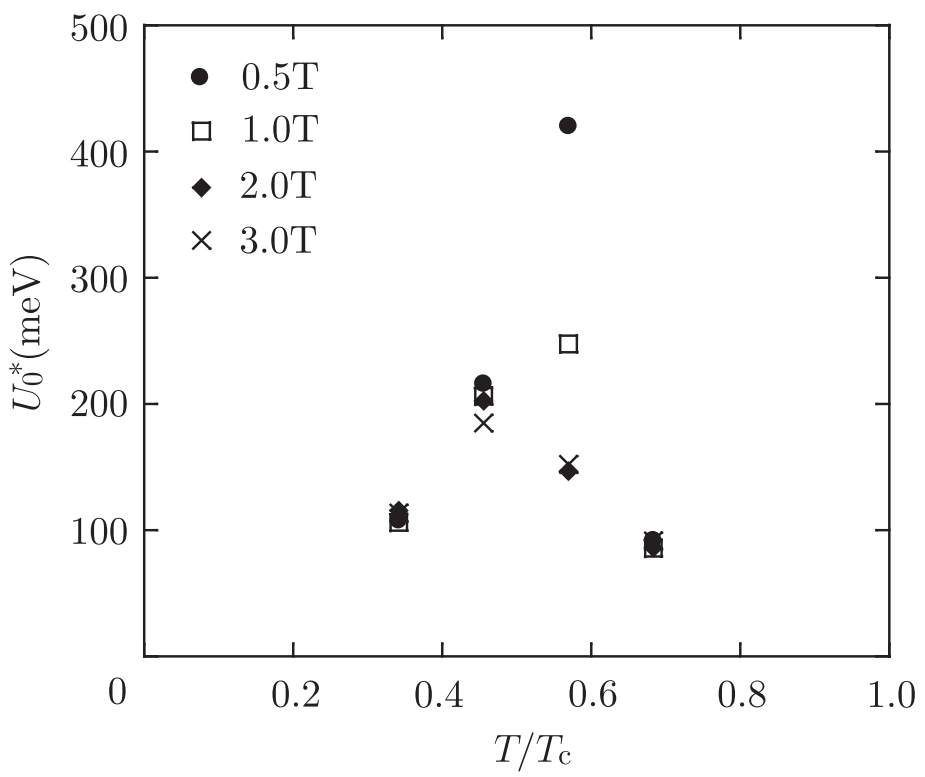


Figure 5: K. Yamauchi *et al.*/WSP-18/ ISS2002